

RESEARCH ARTICLE

Determination of the minority carrier lifetime in crystalline silicon thin-film material

Dominic Walter^{1,2}, Philipp Rosenits¹, Bastian Berger^{3,4}, Stefan Reber¹ and Wilhelm Warta^{1*}

¹ Fraunhofer Institute for Solar Energy Systems, Heidenhofstraße 2, D-79110 Freiburg, Germany

² Now at Institute of Solar Energy Research Hamelin, Am Ohrberg 1, D-31860 Emmerthal, Germany

³ Institute of Theoretical Physics, TU Bergakademie Freiberg, Leipziger Straße 23, D-09596 Freiberg, Germany

⁴ Now at Freiberg Instruments GmbH, Am St. Niclas Schacht 13, D-09599 Freiberg, Germany

ABSTRACT

The effective minority carrier lifetimes on epitaxial silicon thin-film material have been measured successfully using two independent microwave-detected photoconductivity decay setups. Both measurement setups are found to be equally suited to determine the minority carrier lifetime of crystalline silicon thin-film (cSiTF) material. The different measurement conditions to which the sample under investigation is exposed are critically analyzed by both simulations and measurements on a large number of lifetime samples. No systematic deviation between the lifetime results from different measurement setups could be observed, underlining the accuracy of the determined lifetime value. Subsequently, a method to separate the epitaxial bulk lifetime and the total recombination velocity, consisting of front surface and interface recombination between the epitaxial layer and the substrate, is presented. The method, based on different thicknesses of the epitaxial layer, is applied to all batches of this investigation. Each batch consists of samples with the same material quality but different epitaxial layer thicknesses whereas different batches differ in their material quality. In addition, the same method is also successfully applied on individual cSiTF samples. From the results, it can be concluded that the limiting factor of the effective minority carrier lifetime for the investigated solar-grade cSiTF material is the elevated recombination velocity at the interface between epitaxial layer and the substrate compared with microelectronic-grade material. In contrast, the samples cannot be classified into different material qualities by their epitaxial bulk lifetimes. Even on multicrystalline substrate, solar-grade material can exhibit high epitaxial bulk lifetimes comparable to microelectronic-grade material.

Copyright © 2012 John Wiley & Sons, Ltd.

KEYWORDS

minority carrier lifetime; microwave-detected photoconductivity decay; crystalline silicon thin-films

*Correspondence

W. Warta, Fraunhofer Institute for Solar Energy Systems ISE, Heidenhofstraße 2, D-79110 Freiburg, Germany.

E-mail: Wilhelm.Warta@ise.fraunhofer.de

Received 24 October 2011; Revised 12 March 2012; Accepted 20 April 2012

1. INTRODUCTION

Crystalline silicon thin-film material is an attractive alternative to bulk silicon wafers as it provides the opportunity to reduce the starting material costs significantly. Although only a small amount of high-purity silicon is used, remarkably high energy conversion efficiencies of up to 17.6% [1] have already been reported on crystalline silicon thin-film solar cells, consisting of a moderately doped, p-type epitaxial base deposited on a highly doped, p-type, Czochralski (Cz) substrate. Despite these achievements, the electrical characterization, that is, the determination of the minority carrier lifetime, of the two-layer structure remains challenging, as

the two layers cannot be separated physically and therefore must be measured together. Hence, a measurement technique is needed which allows to distinguish the influence of each of the two layers on the measurement signal. Compared with previous lifetime investigations on epitaxial layers, for example by Ogyta [2] and Hara *et al.* [3], this work aims to study the possibility to measure effective lifetimes on this specific p/p⁺ cSiTF material with a variety of different material qualities using commercially available microwave-detected photoconductivity decay (MWPCD) setups.

The samples consist of two differently doped layers, the moderately doped epitaxial layer and the highly doped substrate. Schöfthaler *et al.* [4] showed the dependence of the

measurement signal during an MWPCD measurement on the material's doping concentration and the setup configuration. As the applied MWPCD setups are optimized to investigate standard photovoltaic material with a specific resistivity above $0.1 \Omega\text{cm}$, the transient measurement signals of the specific cSiTF material are dominated by the epitaxial layer, as will be discussed later. This contribution shows the applicability of MWPCD measurements to investigate cSiTF samples with a highly doped substrate and a moderately doped epitaxial layer. Furthermore, the influence of different parameters such as the material quality of the substrate or the thickness of the epitaxial layer on the effective lifetime of the material will be studied. A method to extract the epitaxial bulk lifetime from the measured effective lifetime will be applied to cSiTF samples, allowing the bulk lifetime-related limitations to be separated from the surface/interface-related limitations of the effective lifetime value.

2. INVESTIGATED MATERIAL

The investigated cSiTF material (Figure 1) consists of a highly doped ($n_{\text{sub}} \approx 0.02 \Omega\text{cm}$) p-type substrate, upon which a moderately doped ($n_{\text{epi}} \approx 1 \Omega\text{cm}$) p-type epitaxial layer is deposited via chemical vapor deposition (CVD) at temperatures above 1000°C . The influence of the thickness of the epitaxial layer on the effective minority carrier lifetime is studied by varying the thickness of different samples between 10 and 60 μm . In comparison, the substrate is between 300 and 500 μm thick, depending on the investigated substrate material. Passivation layers, consisting of either SiN_x or Al_2O_3 , on both surfaces of the samples minimize their influence on the effective lifetimes. It has to be mentioned that the passivation of the substrate's surface is of minor importance, as the MWPCD measurement signal is not affected by the rear surface in this specific sample structure. The passivation quality is monitored by 1 Ωcm , p-type, float zone samples without epitaxial layer processed in parallel,

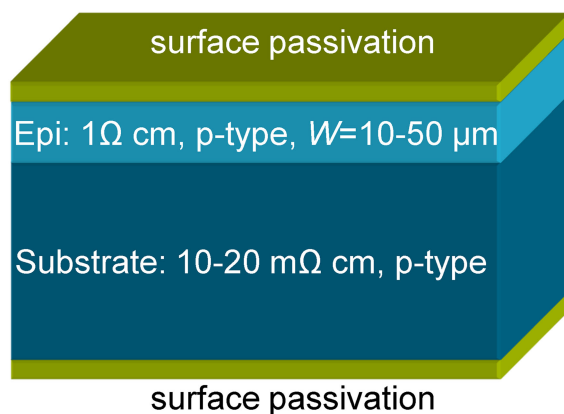


Figure 1. Basic sample structure of crystalline silicon thin-film lifetime samples investigated in this work. For this research, substrate thicknesses between 300 and 500 μm were chosen.

which exhibit surface recombination velocities below 25 cm/s for both types of passivation. It is assumed that the surface of the epitaxial layer exhibits comparable recombination velocity values, whereas the substrate's surface certainly shows a higher recombination because of its elevated doping concentration.

The present study includes different sample qualities: two types of epitaxial layer and three types of underlying substrate. The different epitaxial layer qualities are realized by using different CVD reactors. Some epitaxial layers have been deposited at the Institute of Microelectronics Stuttgart (IMS) in a commercially available barrel-type CVD reactor for microelectronic purposes. In the following, the samples processed at IMS will be referred to as "microelectronic-grade" samples. The epitaxial layers from this reactor are characterized by high material quality and thickness homogeneity throughout the sample. In contrast to these samples, another set of samples has been deposited at the Fraunhofer Institute for Solar Energy Systems ISE in CVD reactors specifically designed for photovoltaic purposes, that is, fast and cost-efficient deposition with relaxed requirements for the homogeneity and material quality compared with microelectronic-grade depositions. The samples processed at ISE will be referred to as "solar-grade" samples. The different substrate qualities used in this contribution are as follows: monocrystalline Cz silicon, multicrystalline (mc) silicon and upgraded metallurgical-grade (umg) silicon. These various materials are classified in four groups consisting of several batches, as shown in Table I.

3. MEASUREMENT SETUP AND PRINCIPLE

To measure the effective minority carrier lifetime of cSiTF samples, two different MWPCD setups are chosen. One of these setups was the well-established WT-2000, distributed by *Semilab Semiconductor Physics Laboratory Co. Ltd.*, and the other was the more recently developed characterization tool MDPmap [5], distributed by *Freiberg Instruments GmbH*. In both setups, the sample under investigation is excited using a laser pulse. The changes to the sample's conductivity, that is, changes of the minority charge carrier density [6], are detected by irradiating a microwave and measuring the changes to either the reflection or absorption of the sample compared with the non-illuminated state. For both setups a microwave frequency v_M in the range of $v_M \approx 10 \text{ GHz}$ is applied. The penetration depth in the moderately doped region is one order of magnitude higher than the epitaxial layer thickness. In the highly doped substrate, however, free carrier absorption occurs and the microwave is absorbed within the first 100 μm . However, this does not affect the measurement as the detectable reflectivity change of the microwave at the substrate vanishes, as it was shown by Schöfthaler *et al.* [4].

In Figure 2, the basic principle of the MWPCD setups is displayed. In performing a measurement, that is, monitoring the time-resolved changes to the photoconductivity (later

Table I. Groups of investigated samples can be divided into different material qualities. Every group, except group “solar-umg,” is represented with several batches in this study. The samples within a batch are processed together to minimize unintended variations in the chemical vapor deposition process. Apart from the material quality and number of batches the surface passivation type and the total number of lifetime measurements of each batch is listed.

Group	Epitaxial layer	Substrate	No. of batches	No. of meas.	Passivation
Micro-mono	Microelectronic-grade	Cz	2	29	$\text{SiN}_x/\text{Al}_2\text{O}_3$
Solar-mono	Solar-grade	Cz	3	52	$\text{SiN}_x/\text{Al}_2\text{O}_3$
Solar-mc	Solar-grade	mc	3	26	SiN_x
Solar-umg	Solar-grade	umg	1	11	SiN_x

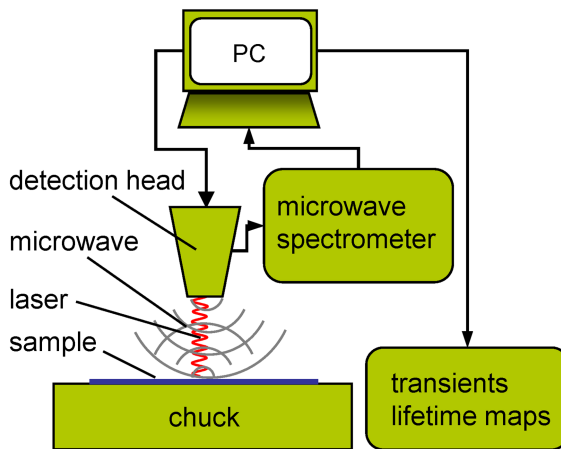


Figure 2. Setup for microwave-detected photoconductivity decay measurements. Compared with WT-2000, MDPmap additionally uses a cavity (not shown) between detection head and sample to detect the conductivity changes.

referred to as transient), an area of $\sim 1 \text{ mm}^2$ is illuminated. The effective minority carrier lifetime can be extracted from the transients by identifying the time constant of the exponential decay after the illumination is switched off. In practice, trapping effects, which hamper the evaluation of the transient, have to be considered. Lateral resolution is achieved by moving the detection head over the sample and performing a measurement on each pixel of the future lifetime map.

Despite having applied the same principle, there are slightly different measurement conditions to which the samples are exposed. As WT-2000 uses a short laser pulse ($t_p = 0.2 \mu\text{s}$), MDPmap features the opportunity to choose much longer pulse widths of the excitation source ($t_p > 100 \mu\text{s}$). With the use of a long pulse, a saturation of the conductivity change can be observed before the exponential decay proceeds. With short excitation pulses, this effect does not occur.

4. SIMULATION RESULTS

To study the differences of the two measurement conditions, the changes to the minority charge carrier density within the

sample during the measurement are simulated by solving the system of the two coupled continuity equations for the epitaxial layer and the substrate, as it was proposed by Väinölä *et al.* [7]. As for all investigated lifetime samples, a highly doped substrate is chosen, the model of Väinölä *et al.* is extended in this work to take band gap narrowing (BGN) in the substrate into account by referring to Schenk [8]. It has to be mentioned that the applied model does not include an additional recombination active surface between the substrate and the epitaxial layer. The simulated transients obtained by this model are in good agreement with Buczkowski *et al.* [9] for the case of a one-layer system. Thus, this approach has been used for an approximate comparison of possible differences resulting from the different measurement conditions for our epitaxial layer system. It has to be noted that the high injection effects in the initial part of a transient are not represented correctly in the described model.

Figure 3 shows the decay of the integrated charge carrier density after the illumination for a cSiTF lifetime sample

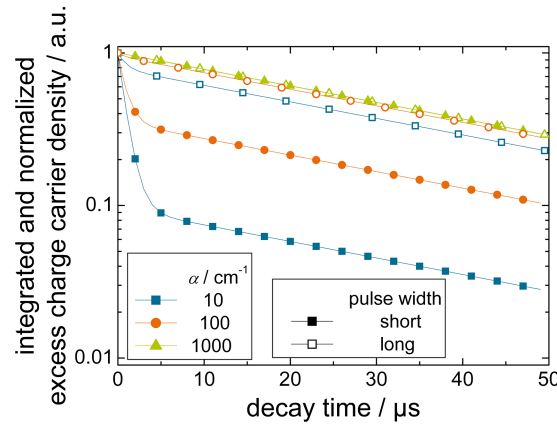


Figure 3. Simulated decay of the excess charge carrier density after excitation. Two different pulse widths, $100 \mu\text{s}$ (long pulse) and $0.2 \mu\text{s}$ (short pulse), are chosen, taking both measurement conditions into account. The simulations are carried out for different wavelengths of the exciting laser. The sample's properties are: $n_{\text{epi}} = 10^{16} \text{ cm}^{-3}$, $n_{\text{sub}} = 2 \times 10^{18} \text{ cm}^{-3}$, $\tau_{\text{epi}} = 100 \mu\text{s}$, $\tau_{\text{sub}} = 1 \mu\text{s}$, $W = 40 \mu\text{m}$, $W_{\text{sub}} = 500 \mu\text{m}$, $S_{\text{front}} = 10 \text{ cm s}^{-1}$, $S_{\text{back}} = 10^4 \text{ cm s}^{-1}$, resulting in an effective minority carrier lifetime of $\tau_{\text{eff}} = 40.1 \mu\text{s}$. The simulated absorption coefficients correspond to a wavelength interval between $\lambda \approx 780 \text{ nm}$ and $\lambda \approx 1060 \text{ nm}$.

with a 40 μm thick epitaxial layer for different excitation wavelengths λ_{ext} , that is, different absorption coefficients α , ranging from 510 nm ($\alpha=10^4 \text{ cm}^{-1}$) to 1060 nm ($\alpha=10 \text{ cm}^{-1}$) [10].

The influence of the measurement condition, that is, the varying pulse width of the excitation laser, can clearly be seen by the different behavior of the transients within the first 5 μs after the laser is switched off. The decay in this period is significantly faster for a short pulse compared with a longer excitation pulse. This discrepancy can be understood by the fact that short excitation pulses lead to a stronger influence of higher modes of the lifetime spectrum in the initial part of the decay compared with long excitation pulses [11]. The effective minority carrier lifetime, defined as the fundamental constant of the decay mode spectrum, can be extracted from the exponential decay when the free carrier distribution has reached the steady state condition [7].

For silicon wafers, the initial part of the transients depends mainly on the front surface recombination velocity (SRV) and the penetration depth of the generation light compared with the later part of the transients, which is influenced by both surface and bulk recombination effects [9] but no longer by the penetration depth. In the case of an epitaxial layer system, as simulated in Figure 3, the front SRV obviously has a minor effect on the transient. This implies that the interface between the epitaxial layer and the substrate, as well as the low lifetime within the substrate, dominate the transient's behavior. As longer wavelengths, that is, low absorption coefficients, penetrate much deeper into the sample ($L_{\text{abs}} (\alpha=10 \text{ cm}^{-1}) \approx 1000 \mu\text{m}$) compared with shorter wavelengths ($L_{\text{abs}} (\alpha=10^4 \text{ cm}^{-1}) \approx 1 \mu\text{m}$) and therefore generate more excess charge carriers in the interface region and the substrate, the fast decay at the beginning of the transient is stronger for small absorption coefficients. In the substrate, the excess charge carriers are assumed to recombine within a shorter time, in the case of Figure 3 with $\tau_{\text{sub}}=1 \mu\text{s}$, compared with $\tau_{\text{epi}}=100 \mu\text{s}$ in the epitaxial layer and therefore contribute to the short strong decay.

This interpretation is supported by the simulations shown in Figure 4, where the substrate's lifetime is varied, keeping all other parameters constant. By lowering the recombination lifetime in the substrate, the period of the strong decay at the beginning of the transient shortens as well. In conclusion, the strong decay at the beginning of the decay transient can be attributed to recombination within the substrate.

Figure 4 also emphasizes the impact of the substrate's electronic quality on the effective lifetime. The drain of minority charge carriers from the epitaxial layer into the substrate depends on the minority carrier lifetime within the substrate as well as on the change of the dopant concentration. Godlewski *et al.* [12] described this inevitable drain at the interface as equivalent to a recombination velocity S_{BSF} . Together with the effects of BGN (also see [13]), the recombination velocity S_{BSF} in the low-level injection regime can be calculated as follows:

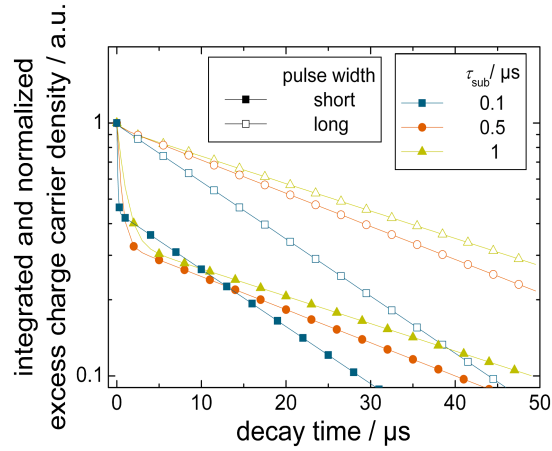


Figure 4. Simulated decay of the excess charge carrier density after 100 ns excitation, for two different pulse widths (100 and 0.2 μs). An excitation wavelength of 978 nm ($\alpha \approx 100 \text{ cm}^{-1}$) is chosen. The varying parameter is the substrate's lifetime τ_{sub} . All other properties correspond to those described in the caption of Figure 3. The resulting effective minority carrier lifetimes are: 40.1, 33.1 and 19.2 μs , from high to low substrate lifetimes, respectively.

$$S_{\text{BSF}} = \frac{D_{\text{sub}}}{L_{\text{sub}} \cdot \Phi} \cdot \frac{\frac{S_{\text{back}} \cdot L_{\text{sub}}}{D_{\text{sub}}} + \tanh \frac{W_{\text{sub}}}{L_{\text{sub}}}}{1 + \frac{S_{\text{back}} \cdot L_{\text{sub}}}{D_{\text{sub}}} \cdot \tanh \frac{W_{\text{sub}}}{L_{\text{sub}}}} \quad (1)$$

with $\Phi = \frac{n_{\text{sub}}}{n_{\text{epi}}} \cdot \exp \left(\frac{\Delta E_{\text{epi}} - \Delta E_{\text{sub}}}{kT} \right)$

Here n_{epi} , n_{sub} , D_{sub} , L_{sub} , S_{back} , W_{sub} , ΔE_{epi} and ΔE_{sub} denote the doping concentration in the epitaxial layer and the substrate, respectively, the diffusion constant and the diffusion length of the minority charge carriers in the substrate, the SRV at the backside of the sample, the width of the substrate and the changes of the Fermi energy in the epitaxial layer and the substrate due to BGN, respectively. k is the Boltzmann constant and T the absolute temperature. It has to be noted that by introducing the effect of BGN into Equation (1), the dependence of S_{BSF} on the substrate's properties change completely. Although without the shift of the energy levels, the recombination velocity would decrease with increasing doping concentration n_{sub} of the substrate, now S_{BSF} increases due to the higher influence of ΔE_{sub} compared with n_{sub} .

In theory, S_{BSF} represents a lower bound of the effective interface recombination velocity S_{eff} . The actually occurring S_{eff} is the sum of S_{BSF} and S_{int} , namely $S_{\text{eff}} = S_{\text{int}} + S_{\text{BSF}}$. S_{int} represents additional recombination via crystallographic defects or impurity atoms at the interface. Figure 5 shows calculated S_{BSF} values for a typical cSiTF sample. The influence of the substrate's doping concentration and its electronic quality can clearly be seen. By lowering the diffusion length within the substrate, the recombination velocity S_{BSF} rises significantly. With the consideration of equal diffusion

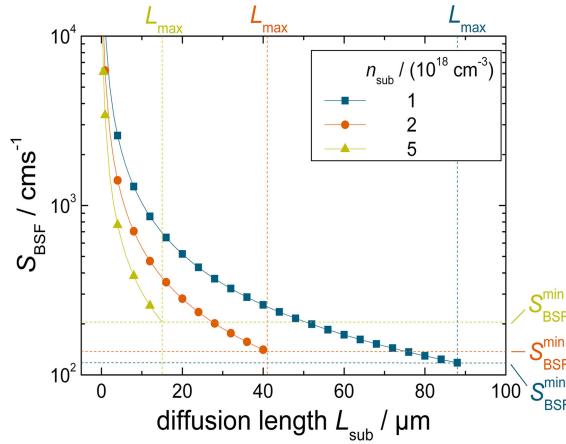


Figure 5. Simulated recombination velocity at the interface between epitaxial layer and substrate for a typical crystalline silicon thin-film sample. The sample's properties are: $n_{\text{epi}} = 5 \times 10^{16} \text{ cm}^{-3}$, $W_{\text{sub}} = 300 \text{ m}$ and $S_{\text{back}} = 10^4 \text{ cms}^{-1}$. Band gap narrowing is included from the model proposed by Schenk [8], whereas the diffusion constants are taken from the photovoltaic simulation tool PC1D [14]. The maximum diffusion length within the substrate L_{max} is defined by the intrinsic lifetime limit.

lengths, the sample with the largest ratio of doping concentrations in the epitaxial layer and the substrate exhibits the smallest S_{BSF} . If high diffusion lengths can be expected, that is, the diffusion length reaches the intrinsic limit, an optimum of the doping concentration ratio exists, resulting in the smallest recombination velocity value $S_{\text{BSF}}^{\text{min}}$. As will be shown later experimentally, this optimization is not required, as the calculated minimum recombination velocity $S_{\text{BSF}}^{\text{min}}$ is for all samples much smaller than the experimentally extracted recombination velocity value.

In summary, the MWPCD simulations assert that the effective lifetimes are expected to be equal in any case and independent of the measurement conditions. Additionally, MWPCD measurements on cSiTF material are preferably to be carried out using a short excitation wavelength, if a well-passivated surface can be realized. In this case, the strong decay at the beginning of the transients is minimized, and the asymptotic decay, characterizing the effective lifetime, is reached faster. A long excitation pulse diminishes the influence of higher modes in the investigated material.

5. MEASUREMENT RESULTS

To compare the simulated transients, that is, the temporal changes of the excess charge carrier density, with the measured transients, that is, the temporal changes of the reflectivity (or absorption) of the irradiated microwave, it has to be kept in mind that in the applied setups for highly doped substrate, the detectable reflectivity changes vanish [4]. Therefore, the strong decay at the beginning of the simulated transients, which is mainly due to the excess

charge carrier density changes within the substrate, is not expected to be observed. Figure 6 shows two typical measured transients using a long and a short excitation pulse. Although there are differences in the shape of the decay transients, both measured transients result in a comparable asymptotic decay constant, if a variable offset $U_1(t)$ on the signal is taken into account. The fitting function to extract the effective minority carrier lifetime therefore reads as follows:

$$U(t) = U_0 \cdot \exp\left(-\frac{t}{\tau_{\text{eff}}}\right) + U_1(t) \quad (2)$$

If this variable offset is deducted correctly, the decay has the shape of a strictly mono-exponential decay in the logarithmic scale.

As expected, no strong decay at the beginning of the transients can be observed. In general, the transients after the short excitation pulse show a slightly increased initial decay compared with the transient after long excitation. By comparing both measurements, it can be concluded that the asymptotic limit is reached comparably fast, suggesting that both long and short pulse measurements are equally suited to extract effective lifetimes of cSiTF samples.

MWPCD measurements were carried out on lifetime samples of all groups shown in Table I using both experimental setups. Apart from group “micro-mono,” it is expected that the epitaxial layer grows non-homogeneously on the substrate, leading to spatial distribution of the effective lifetime over the sample. To take these variations into account, effective lifetime maps were taken. Figure 7 shows two lifetime maps of an mc sample recorded with MDPmap ($t_p = 5 \mu\text{s}$, $\lambda_{\text{ext}} = 978 \text{ nm}$) and WT-2000 ($t_p = 0.2 \mu\text{s}$, $\lambda_{\text{ext}} = 904 \text{ nm}$). The maps have different resolutions; the MDPmap on the left has a resolution of 0.2 mm compared with the WT-2000 map with a resolution of 0.5 mm. The sample's dimension is $50 \times 65 \text{ mm}^2$, but the epitaxial layer is only deposited on a $50 \times 50 \text{ mm}^2$ area in the center of the

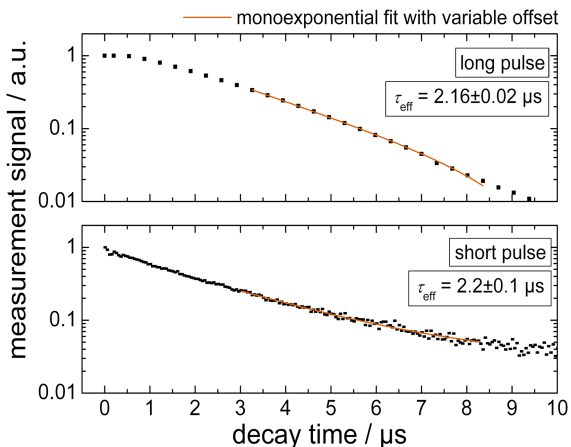


Figure 6. Comparison of two measured decay transients using the measurement setup of MDPmap (top) and of WT-2000 (bottom).

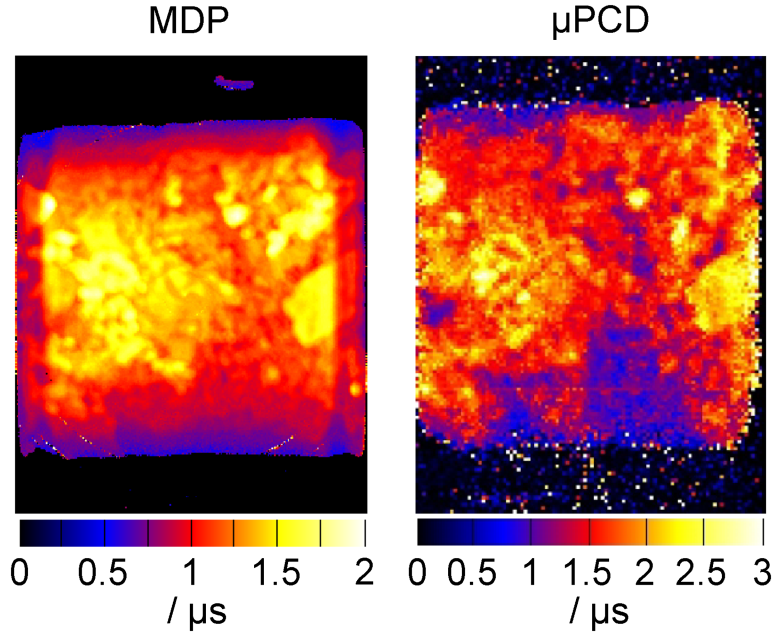


Figure 7. Comparison of two effective lifetime maps recorded from the same crystalline silicon thin-film lifetime sample of batch "solar-mc 1" with $W=45\text{ }\mu\text{m}$. Left: long excitation pulse (MDPmap), right: short excitation pulse (WT-2000). Because of the two different measurement setups, the maximum excess charge carrier density is in the range of $\Delta n=10^{17}\text{ cm}^{-3}$ for MDPmap and $\Delta n=10^{18}\text{ cm}^{-3}$ for WT-2000 [15].

sample. Referring to the dark areas on the top and bottom of the lifetime maps, it can be seen that lifetimes on highly doped materials cannot be measured using these setups. On the measurable center area, both lifetime maps exhibit a comparable mean effective lifetime, determined through arithmetic averaging, of $\tau_{\text{eff}}(\text{MDPmap}) \approx 1.1\text{ }\mu\text{s}$ and $\tau_{\text{eff}}(\text{WT-2000}) \approx 1.5\text{ }\mu\text{s}$, although on the right lifetime map, a higher variation of lifetime values implied a different scaling. This difference may be due to different injection levels or influenced by degradation effects, as a period of 6 months separated the two measurements. As will be shown later, this deviation is not systematic between both measurement setups. Despite these differences, by comparing the visible grain structure, it can be concluded that there is a reasonable agreement between both measurements.

Figure 8 shows all measured average effective lifetime values of this investigation, measured with both MWPCD setups, plotted against the average epitaxial layer thickness. It is obvious that, for all sample groups, the effective lifetime is increasing with increasing layer thickness. To explain this behavior, either (i) the bulk lifetime within the epitaxial layer τ_{epi} must depend on the layer thickness, or (ii) this increase may be due to the diminishing influence of the surface and/or interface on the effective lifetime. An increase of τ_{epi} seems unlikely, as from the technological point of view, an increase of the epitaxial layer thickness should rather lower the bulk lifetime (because, for example, the sample is exposed longer to the elevated temperatures during deposition). Therefore, the slope of the effective lifetime with increasing layer thickness is attributed to the influence of the surface and the interface. Judged from float zone wafers

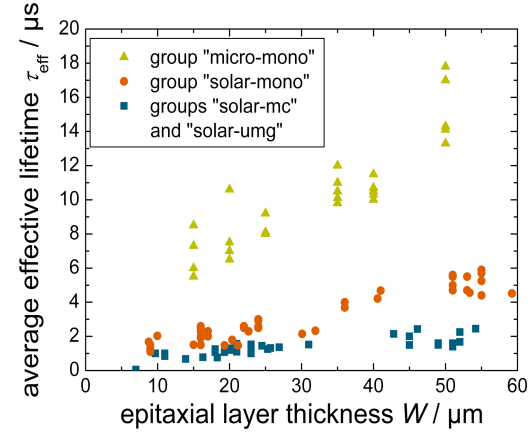


Figure 8. Performed measurements on all crystalline silicon thin-film lifetime samples of this investigation divided into three different groups. The measured effective lifetime is plotted against the average epitaxial layer thickness.

processed in parallel, the front surfaces of all samples are well passivated, so that the reason for the increase may be further restricted to effects related to the interface between epitaxial layer and substrate. For the specific sample structure of the investigated samples, it can be calculated that the minimum recombination velocity at the interface is one order of magnitude higher than the SRV at the front surface. The three different slopes for samples of different groups suggest that different groups differ in their recombination velocity at the interface.

Measurements using different excitation wavelengths were performed for all samples of each group with both measurement setups (Table I). The excitation wavelengths are $\lambda_{\text{ext}} = 660 \text{ nm}$ and $\lambda_{\text{ext}} = 978 \text{ nm}$ for MDPmap and $\lambda_{\text{ext}} = 350 \text{ nm}$, $\lambda_{\text{ext}} = 532 \text{ nm}$ and $\lambda_{\text{ext}} = 904 \text{ nm}$ for WT-2000. Figure 9 shows exemplarily the result for the group “solar-mono.” The plotted values correspond to the average epitaxial layer thickness and the average effective minority carrier lifetime of each individual cSiTF sample. It can be seen that no systematic variation regarding the measurement setup and excitation wavelength can be observed. This applies to all investigated samples and affirms the theoretical prediction.

The separate determination of S_{eff} at the interface and the bulk lifetime τ_{epi} within the epitaxial layer is of great interest and will be performed in the following as proposed by Faller [16].

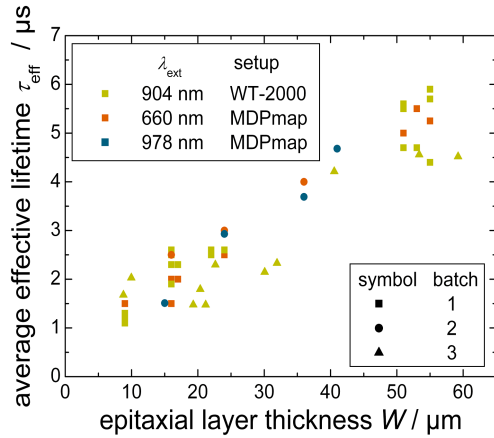


Figure 9. Measured effective lifetimes of group “solar-mono” divided into the three contained batches, different applied excitation wavelengths and setups.

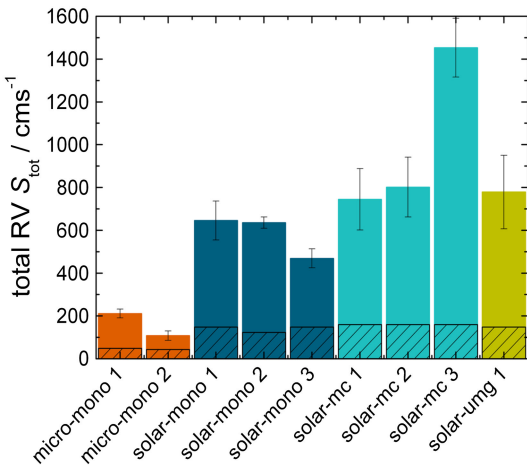
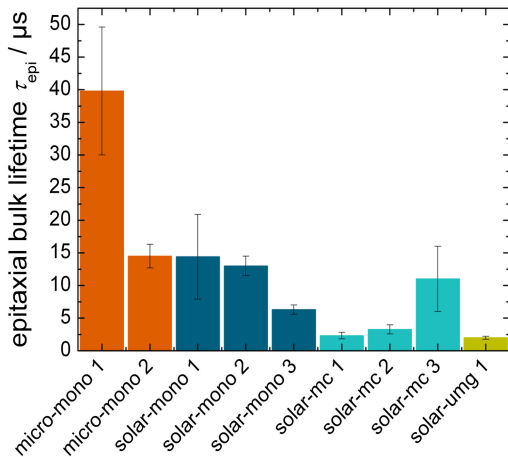


Figure 10. Epitaxial bulk lifetimes (left) and total recombination velocities (right) for the different batches of this study. The shaded areas on the right represent the minimum interface recombination velocity calculated with the specific sample properties and Equation (1).

For all cSiTF lifetime samples in this study, the condition $S_{\text{tot}} < D_{\text{epi}}/(4W)$ (W being the epitaxial layer thickness) is fulfilled. Therefore, the following equation introduced by Sproul *et al.* [17] can be applied:

$$\frac{1}{\tau_{\text{eff}}} = \frac{1}{\tau_{\text{epi}}} + \frac{S_{\text{tot}}}{W} = \frac{1}{\tau_{\text{epi}}} + \frac{S_{\text{front}} + S_{\text{eff}}}{W} \\ = \frac{1}{\tau_{\text{epi}}} + \frac{S_{\text{front}} + S_{\text{BSF}} + S_{\text{int}}}{W} \quad (3)$$

In this case, S_{front} denotes the SRV at the front surface.

With the assumption of the epitaxial layer thickness in each batch to be the only varying parameter, τ_{epi} and the total recombination velocity (RV) S_{tot} may be extracted from a $\tau_{\text{eff}}^{-1}(W^{-1})$ -plot, where the y-axis intercept equals the inverse lifetime in the layer and the slope equals S_{tot} . This analysis is applied to every batch listed in Table I and its result is shown in Figure 10. On the left the epitaxial bulk lifetimes and on the right the total RV S_{tot} for all batches is displayed. To identify additional recombination apart from S_{BSF} , Figure 10 also displays the calculated minimum values of the interface recombination velocity $S_{\text{BSF}}^{\text{min}}$ (shaded areas in the right diagram) calculated from Equation 1, assuming an intrinsically limited diffusion length in the substrate. For the calculation, the values $L_{\text{sub}} = 31.4 \mu\text{m}$ for the batches micro-mono 1 and solar-mono 2, $L_{\text{sub}} = 23.9 \mu\text{m}$ for batch micro-mono 2 and $L_{\text{sub}} = 19.3 \mu\text{m}$ for all other batches are chosen.

It can be concluded that every sample group suffers from additional recombination. This additional recombination can be caused by either crystal defects and impurity atoms or a significant degradation of the substrate material during the CVD process. Different sample groups show different characteristics. Group “micro-mono” exhibits high epitaxial bulk lifetimes above $10 \mu\text{s}$ and low recombination velocities at the interface, safely below 250 cm/s . By looking at the groups processed at Fraunhofer ISE, an

interesting observation is that it is possible to achieve high lifetime values on monocrystalline substrate and even on multicrystalline substrates (batch “solar-mc 3”) comparable to group “micro-mono.” However, three batches with mc substrates exhibiting a significantly lower lifetime indicate the sensitivity of the process and the dependence on the substrate’s purity. By comparing the solar-grade groups with group “micro-mono,” it is obvious that the main difference between the microelectronic-grade and solar-grade samples is the different recombination velocity at the interface. Apart from one exception (solar-mono 3), all solar-grade samples exhibit high recombination velocities above 600 cm/s. These higher recombination velocities may be attributed to a higher density of defects at the interface or a degradation of the substrate material during CVD deposition. By separating the effective lifetime into the epitaxial bulk lifetime and the total recombination velocity, it can be concluded that the effective lifetime of our solar-grade cSiTF samples is not limited by the epitaxial bulk lifetime but rather by recombination effects at the interface. A reduction of the defect density at the interface is desirable in order to improve the electrical quality of solar-grade samples. For this purpose, an enhanced predeposition surface clean of the substrate should be studied.

The results shown in Figure 10 are based on all samples of one batch each with a different average epitaxial layer thickness. As mentioned before for solar-grade samples, a distribution of the layer thickness over the sample’s surface is expected and measurable. This thickness distribution can be exploited to extract the epitaxial bulk lifetime for every individual cSiTF sample if a $\tau_{\text{eff}}^{-1}(W^{-1})$ -plot can be realized. This approach bears two major advantages: on the one hand, only one cSiTF lifetime sample needs to be processed to achieve information about the epitaxial bulk lifetime and the interface recombination, and on the other hand, the assumption can be relaxed that all parameters except the epitaxial layer thickness are constant within one batch (especially that the epitaxial bulk lifetime has to remain unchanged between different samples). Figure 11 shows the $\tau_{\text{eff}}^{-1}(W^{-1})$ -plot for batch “solar-mono 3.” For three samples of this batch, the lateral thickness distribution of the epitaxial layer has been determined by exploiting stacking faults [18]. The thickness distribution has been correlated with lifetime maps, which were previously measured. For comparison, the average values for each sample of batch “solar-mono 3” are displayed as well (black stars). As indicated by the two different fits in Figure 11, comparable values for the epitaxial bulk lifetime, $\tau_{\text{epi}} = 5.6 \pm 0.2 \mu\text{s}$ for the fit of three samples and $\tau_{\text{epi}} = 6.3 \pm 0.7 \mu\text{s}$ for the whole batch, and only slightly different total recombination velocity values of $S_{\text{tot}} = 565 \pm 19 \text{ cm/s}$ and $S_{\text{tot}} = 496 \pm 44 \text{ cm/s}$, again for the three-sample fit and the whole batch, respectively, can be extracted. The inaccuracies of the extracted values are of statistical nature. For each lifetime value, a relative inaccuracy of 10% of each numerical value has been estimated. From the comparable extracted values, it can be concluded that in order to minimize the complexity of the process to determine the epitaxial bulk lifetime and the total recombination velocity, a measurement

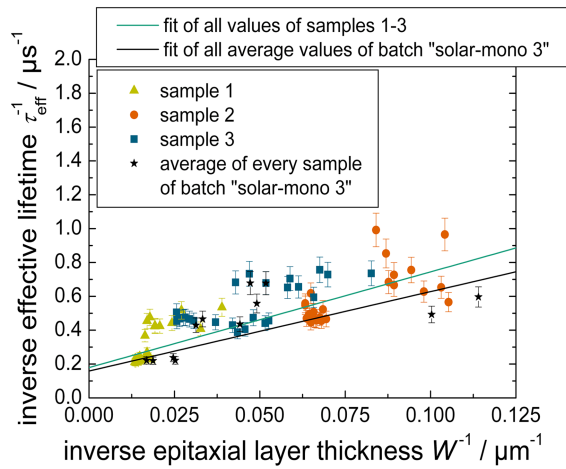


Figure 11. $\tau_{\text{eff}}^{-1}(W^{-1})$ -plot for batch “solar-mono 3.” Every star indicates the average value of one crystalline silicon thin-film lifetime sample. The behavior of the average value is compared with the behavior of spatial resolved measurements on three different lifetime samples of the same batch.

on a single-cSiTF sample can be performed with reasonable accuracy.

6. SUMMARY

In summary, it can be said that measurements of the effective minority carrier lifetime on crystalline silicon thin-film (cSiTF) samples can reliably be performed using microwave detected photoconductivity decay (MWPCD) measurements. Two different MWPCD setups, which mainly differ in the duration of the generation pulse, have been studied analytically and experimentally. No deviation between the results from both setups with regard to the extracted effective lifetime can be observed. Recently, the MDPmap setup has been further improved, now allowing measurements to be performed with short excitation pulse lengths comparable to the WT-2000 tool.

Subsequently, an approach to separate the epitaxial bulk lifetime and the total recombination velocities has been presented and applied to a large number of cSiTF samples in two different ways. Firstly, the epitaxial bulk lifetime τ_{epi} and the total recombination velocity S_{tot} have been extracted for a whole batch comprising layers of widely varying thicknesses. The average effective minority carrier lifetime and the average epitaxial layer thickness of each sample in the investigated batch were used. Secondly, the thickness distribution of three different samples has been exploited to extract τ_{epi} and S_{tot} . A comparison of both methods underlines the applicability of the presented method, not only on a batch consisting of a large number of cSiTF samples, but also on a single sample if it exhibits a measurable layer thickness distribution.

On the basis of the findings, it can be concluded that the investigated epitaxial layers from microelectronic-grade and

solar-grade lifetime samples exhibit different total recombination velocities $S_{\text{tot}}^{\text{micro}} \leq 250 \text{ cm/s}$ and $S_{\text{tot}}^{\text{solar}} \geq 500 \text{ cm/s}$. In contrast, both cSiTF material qualities cannot be distinguished by the extracted epitaxial bulk lifetime. Even on mc substrate, bulk lifetimes comparable to microelectronic-grade samples on Cz substrates can be achieved. Nevertheless, the tendency can be identified, which solar-grade samples, especially on multicrystalline and upgraded metallurgical-grade substrates, tend to show reduced lifetimes compared with the microelectronic-grade samples.

ACKNOWLEDGEMENTS

The authors thank the Fraunhofer-Gesellschaft for internal project funding in the frame of the “Si-Beacon” project. This work was also financially supported by the European Social Funds (ESF) 2007–2013 with the project number 080940489 and the state of Saxony.

REFERENCES

1. Faller FR, Henninger V, Hurrel A, Schillinger N. *Optimization of the CVD process for low-cost crystalline-silicon thin-film solar cells*. Proceedings of the 2nd World Conference on Photovoltaic Energy Conversion, Vienna, Austria 1998; 1278–83.
2. Ogita Y. Non-contact observations of photoconductivity decay and carrier lifetime measurements in epitaxial silicon wafers. *Semiconductor Science and Technology* 1992; **7**: A175–A179.
3. Hara T, Tamura F, Kitamura T. Minority carrier lifetime measurements in epitaxial silicon layers. *Journal of the Electrochemical Society* 1997; **144**: L54–L57.
4. Schöfthaler M, Brendel R. Sensitivity and transient response of microwave reflection measurements. *Journal of Applied Physics* 1995; **77**(7): 3162–73.
5. Berger B, Schüler N, Angerer S, Gründick-Wendrock B, Niklas JR, Dornich K. Contactless electrical defect characterization in semiconductors by microwave detected photo induced current transient spectroscopy (MD-PICTS) and microwave detected photoconductivity (MDP). *Physica Status Solidi A* 2011. DOI: 10.1002/pssa.201083994
6. Kunst M, Beck G. The study of charge carrier kinetics in semiconductors by microwave conductivity measurements. *Journal of Applied Physics* 1986; **60**(10): 3558–66.
7. Väinölä H, Storgårds J, Yli-Koski M, Sinkkonen J. Evaluation of effective carrier lifetime in epitaxial silicon layers. *Solid State Phenomena* 2002; **82–84**: 771–76.
8. Schenk A. Finite-temperature full random-phase approximation model of band gap narrowing for silicon device simulation. *Journal of Applied Physics* 1998; **84**(7): 3684–95.
9. Buczkowski A, Radzimski ZJ, Rozgonyi GA, Shimura F. Separation of the bulk and surface components of recombination lifetime obtained with a single laser/microwave photoconductance technique. *Journal of Applied Physics* 1992; **72**(7): 2873–78.
10. Green MA, Keevers MJ. Optical properties of intrinsic silicon at 300 K. *Progress in Photovoltaics: Research and Applications* 1995; **3**(3): 189–92.
11. Luke KL, Cheng LJ. Analysis of the interaction of a laser pulse with a silicon wafer: determination of bulk lifetime and surface recombination velocity. *Journal of Applied Physics* 1987; **61**(6): 2282–93.
12. Godlewski MP, Baraona CR, Brandhorst HW. *Low-high junction theory applied to solar cells*. Proceedings of the 10th IEEE Photovoltaic Specialists Conference, Palo Alto, California, USA 1973; 40–9.
13. Rohatgi A, Rai-Choudhury P. Design, fabrication and analysis of 17–18 percent efficient surface-passivated silicon solar cells. *IEEE Trans. Electron Devices* 1984; **ED-31**(5): 596–601.
14. Clugston DA, Basore PA. *PC1D version 5: 32-bit solar cell modeling on personal computers*. Proceedings of the 26th IEEE Photovoltaic Specialists Conference, Anaheim, California, USA 1997; 207–10.
15. Walter D, Rosenits P, Kopp F, Reber S, Berger B, Warta W. *Determination of the minority carrier lifetime in epitaxial silicon layers by microwave-detected photoconductivity measurements*. Proceedings of the 5th World Conference on Photovoltaic Energy Conversion, Valencia, Spain 2010; 2078–83.
16. Faller FR. Epitaxial silicon thin-film solar cells. Dissertation, Universität Freiburg 1998.
17. Sproul AB. Dimensionless solution of the equation describing the effect of surface recombination on carrier decay in semiconductors. *Journal of Applied Physics* 1994; **76**(5): 2851–4.
18. Aharoni H. Stacking-faults in silicon epitaxial layers. *Vacuum* 1976; **26**(4–5): 167–80.